

On the Bistable Behavior of a Low-Frequency Raman-Active Phonon Line in Superconducting Oxide $\text{Ba}_{1-x}\text{K}_x\text{BiO}_3$

A. P. Saiko* and S. A. Markevich

Institute of Solid-State and Semiconductor Physics, National Academy of Sciences of Belarus, Minsk, 220072 Belarus

**e-mail: saiko@iftp.bas-net.by*

The two-loop temperature hysteresis of integrated intensity of Raman scattering of light is explained theoretically for a line of frequency 50 cm^{-1} in a superconducting oxide $\text{Ba}_{1-x}\text{K}_x\text{BiO}_3$ single crystal.

PACS numbers: 74.25.Kc; 74.25.Gz

The cuprate-free superconductor $\text{Ba}_{1-x}\text{K}_x\text{BiO}_3$ (BKBO) with the superconducting transition temperature $T_c \approx 32 \text{ K}$ (for samples with $x \approx 0.37$) occupies a special place among high-temperature oxide superconductors. Superconducting BKBO compounds crystallize into a cubic perovskite structure, do not contain an analog of the CuO_2 layers inherent in cuprates, are diamagnetic, and do not possess a static magnetic order. Although the considerable isotopic effect and the superconducting gap width match the results of the standard BCS model, other mechanisms of the formation of the superconducting state (in addition to the phonon mechanism) should be employed for explaining high values of T_c and low densities of states of charge carriers.

It has been generally accepted [1] that the unique properties of these compounds are determined to a considerable extent by the dynamics and the electron structure of BiO_6 octahedra. The vibrational spectrum of BKBO strongly depends on the dopant (potassium) concentration x ; however, all samples with different values of x exhibit a phonon vibration at a frequency of 50 cm^{-1} . This line appears in the Raman spectra for the XX polarization owing to the R type rotational distortion [2]. The line intensity is maximal for metallic samples with $x \approx 0.33$ and exhibits an intriguing feature, i.e., two-loop hysteretic behavior as a function of temperature in the range $10\text{--}200 \text{ K}$ [2]. It is interesting to note that latticed instability with a strong softening of elastic moduli, as well as hysteretic temperature behavior for samples with $x \approx 0.37$ (which was discovered with the help of ultrasonic measurements [3]), is observed in the same temperature range.

It will be shown below that the existence of the 50-cm^{-1} line in the Raman spectra and that its bistable behavior can be explained using existing concepts of the dynamics of building blocks of the BKBO crystal

lattice, i.e., BiO_6 octahedra, as well as their electronic structure.

It was found [4] that there exist two types of BiO_6 octahedra with two different lengths of the Bi–O bond and rigidities. The crystal structure of the parent compound BaBiO_3 is formed by alteration of expanded (soft) and compressed (hard) BiO_6 octahedra. The electronic structures of soft and hard octahedra are also different. In a soft BiO_6 octahedron, 2 antibonding orbitals are completely filled with 20 electrons, while such orbitals in a hard BiL^2O_6 octahedron are filled with 18 electrons and a free energy level (hole pair L^2) is present in the upper antibonding orbital. Doping of BaBiO_3 with potassium is equivalent to addition of holes and leads to partial replacement of large soft octahedra by small hard ones. This results in a decrease in the number of static breather and rotational distortions and their gradual disappearance. According to neutron diffraction data [5], the structure of the compound ultimately becomes, on average, cubic for a doping level of $x \geq 0.37$. However, the EXAFS analysis of the four nearest spheres in the bismuth surroundings for samples with $x \geq 0.37$ indicates local rotations of octahedra through $4^\circ\text{--}5^\circ$ [6], while Raman spectra indicate that the symmetry becomes lower as compared to simple cubic symmetry [7]. Moreover, it was found [1, 8] that oxygen ions belonging simultaneously to BiO_6 and BiL^2O_6 octahedra vibrate in a two-well asymmetric potential, while oxygen ions belonging to identical BiL^2O_6 octahedra vibrate in a simple harmonic potential. The two-well shape of the potential is due to different fillings of the upper antibonding orbital in BiO_6 and BiL^2O_6 octahedra. During tunneling of an oxygen ion from one well to the other, an electron pair simulta-

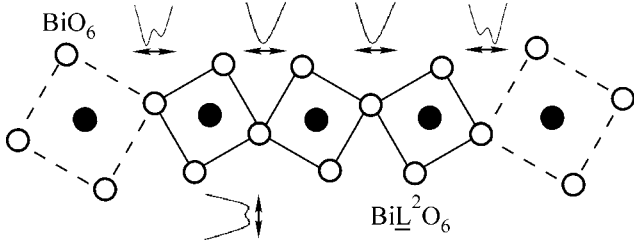


Fig. 1. Schematic representation of a cooperated complex of octahedra in the BiO_2 plane in the $[100]$ direction (see text); dark circles correspond to Bi and light circles, to O.

neously passes from a BiO_6 octahedron to a BiL^2O_6 octahedron; accordingly, these octahedra exchange their roles (i.e., the dynamic exchange $\text{BiO}_6 \longleftrightarrow \text{BiL}^2\text{O}_6$ takes place). In [1], superconductivity in bismuth-containing compounds is regarded as movement of local electron pairs of this type.

With increasing doping level, the number of BiL^2O_6 octahedra increases and, for $x \geq 0.33$, the lattice acquires three-dimensional complexes, i.e., spatially overlapping BiL^2O_6 octahedra. The free energy level in these complexes expands to form the conduction band, and metal-type conductivity is formed when the energy of localization of electron pairs becomes equal to zero [1]. As a result, all octahedra in a complex can perform coherent rotational vibrations (e.g., around the $[001]$ axis). Figure 1 shows such a complex schematically in the BiO_2 plane of octahedra along the $[100]$ direction. The dynamic exchange by the roles of octahedra $\text{BiO}_6 \longleftrightarrow \text{BiL}^2\text{O}_6$, which is realized due to the escape of an oxygen ion from the global minimum of the asymmetric two-well potential and the transfer of an electron pair to a BiL^2O_6 octahedron, is complicated in this case since it would require mismatching of the cooperative movement of the entire complex of BiL^2O_6 octahedra. Cooperativity first leads to suppression of fluctuation-induced jumps of an oxygen ion from the global minimum to a local one upon heating of the system to a certain temperature. Second, matched rotational vibrations of the octahedra in the complex, which locally distort the cubic perovskite structure, may become Raman-active (this is actually observed for vibrations at a frequency of 50 cm^{-1}). The emergence of local distortions of cubic structure due to correlated rotational vibrations of octahedra in the entire complex of this type can be treated as a locally realized phase transition of displacement type (the symmetric potential with two shallow minima in the $[010]$ direction in Fig. 1 confirms this statement).

We will consider the emergence of local distortions and lattice instability in rotational distortions of octahe-

dra about the $[001]$ axis by using the Hamiltonian

$$H = \sum_l \left(\frac{P_l^2}{2M} + \frac{Mv_o^2}{2} Q_l^2 + \frac{B}{4} Q_l^4 \right) - \frac{1}{2} \sum_{l \neq l'} v_{ll'} Q_l Q_{l'}, \quad (1)$$

where v_o is the local frequency of small oscillations in the absence of interactions ($v_o = 50 \text{ cm}^{-1}$ in our case), Q_l is the generalized coordinate describing the rotation of octahedra, B is the anharmonicity constant, $v_{ll'}$ are the interaction constants, and M is the mass. We choose the asymmetric two-well potential for describing the motion of oxygen ion belonging to BiO_6 and BiL^2O_6 octahedra in the form

$$V = \frac{\alpha}{2} q^2 - \frac{\beta}{3} q^3 + \frac{\gamma}{4} q^4, \quad (2)$$

where α , β , and $\gamma (>0)$ are constants and q is the generalized coordinate of the ion. Vibrations of octahedra depend on the position of oxygen ions in the two-well potential. This can be accounted for by introducing the cubic and quartet terms of the interaction,

$$H_{\text{int}}^{(3)} = q^2 \sum_k \lambda_k^{(3)} Q_k, \quad H_{\text{int}}^{(4)} = q^2 \sum_{k, k'} \lambda_{k, k'}^{(4)} Q_k Q_{k'}, \quad (3)$$

where Q_k are the Fourier components of coordinates Q_l and $\lambda_k^{(3)}$ and $\lambda_{k, k'}^{(4)}$ are the coupling coefficients. We can represent the renormalization of the initial frequency ($v_o \rightarrow v_r$) in the self-consistent phonon approximation in the fourth-order interaction in Hamiltonian (1) and in the first and second approximations in perturbation theory in $H_{\text{int}}^{(4)}$ and $H_{\text{int}}^{(3)}$, respectively, in the form

$$v_r^2 = v_o^2 + \frac{3B}{M_{\text{eff}}} (\langle Q \rangle^2 + \langle \delta Q^2 \rangle) + \frac{2\lambda_{k, k'}^{(4)}}{M_{\text{eff}}} (\langle q \rangle^2 + \langle \delta q^2 \rangle) - \frac{(\lambda_k^{(3)})^2}{mM_{\text{eff}}\Omega^2} (4\langle q \rangle^2 + \langle \delta q^2 \rangle). \quad (4)$$

(see also [9,]). Here, $\langle Q \rangle$ and $\langle \delta Q^2 \rangle = \langle (Q - \langle Q \rangle)^2 \rangle$ are the mean statistical values of the coordinate and its variance ($\langle q \rangle$ and $\langle \delta q^2 \rangle$ have an analogous meaning), M_{eff} is the effective mass of the complex of octahedra generating local distortion $\langle Q \rangle$ (a complex may have a linear size of four to six octahedra), and $\Omega^2 = \frac{1}{m} [\alpha - 2\beta\langle q \rangle + 3\gamma(\langle q \rangle^2 + \langle \delta q^2 \rangle)]$ is the oxygen ion frequency in the two-well potential. The mean values $\langle q \rangle$ and $\langle \delta q^2 \rangle$ can be determined self-consistently from the equations

$$\langle \delta q^2 \rangle = \frac{1}{2m\Omega} \coth \frac{\Omega}{2\theta}, \quad (5)$$

$$(\beta - 3\gamma\langle q \rangle) \langle \delta q^2 \rangle = \alpha\langle q \rangle - \beta\langle q \rangle^2 + \gamma\langle q \rangle^3,$$

while $\langle Q \rangle$ and $\langle \delta Q^2 \rangle$ can be determined from the equations

$$\langle \delta Q^2 \rangle = \frac{\theta}{M_{\text{eff}} v_r^2}, \quad (6)$$

$$M_{\text{eff}} v_o^2 + 3B \langle \delta Q^2 \rangle + B \langle Q \rangle^2 - v = 0,$$

where $v = \sum_r v_{lr}$, m is the mass of an oxygen ion, and $\theta = k_B T$. In deriving Eq. (4), we took into account the fact that the vibrational frequency of octahedra is much smaller than the frequency of oxygen ions. For the temperature range we are mainly interested in, we have $k_B T \gg v_o$; for this reason, for simplicity, variance $\langle \delta Q^2 \rangle$ is represented by the classical formula in relations (6). The value of M_{eff} can be determined by comparing the local phase transition temperature T_o , estimated by formula $k_B T_o \approx M_{\text{eff}} v_o^2 \langle Q \rangle_{\text{max}}^2$, with the experimentally measured value T_o^{exp} . Since $\langle Q \rangle_{\text{max}} \approx 0.15 \text{ \AA}$ for rotation of octahedra through 5° for a lattice constant $a \approx 4.3 \text{ \AA}$ and $T_o^{\text{exp}} \approx 300 \text{ K}$ [2], we obtain an estimate of $M_{\text{eff}} \approx 800m$; i.e., the complex consists of 200 octahedra and occupies a region of approximately $25 \times 25 \times 25 \text{ \AA}^3$. Parameters α , β , and γ of potential (2) can be estimated on the basis of EXAFS data, i.e., from a potential barrier height of $\sim 0.026 \text{ eV}$ and the local maximum and local minimum coordinates ~ 0.075 and $\sim 0.15 \text{ \AA}$, respectively [8].

For crystals with a perovskite cubic structure, principal-order terms in the power expansion of polarizability in Raman-active modes are absent in view of the symmetry and the main contribution to the Raman scattering tensor comes from second-order terms. For this reason, we can express the integrated intensity of light scattering in the form

$$I \sim \langle Q \rangle^2 \langle \delta Q^2 \rangle = \langle Q \rangle^2 \frac{\theta}{M_{\text{eff}} v_r^2} \quad (7)$$

or, taking into account the second equation in (6), we can write the reduced intensity in the form

$$\frac{I}{\theta} \sim \frac{\langle Q \rangle^2}{2B \langle Q \rangle^2 + v}. \quad (8)$$

At temperatures higher than the critical temperature T_o of a local phase transition of the displacement type, we have $\langle Q \rangle = 0$ and, in accordance with formula (8), intensity $I = 0$. After the emergence of local distortions $\langle Q \rangle^2 \sim T_o - T$, intensity in the temperature range $T < T_o$ differs from zero and increases upon cooling. The temperature dependence of reduced intensity I/θ calculated using formulas (8) and (4)–(6) is in qualitative agreement with the experimental curve (Fig. 2). Obviously, the temperature hysteresis in the form of a two-loop curve is due to temperature renormalization of fre-

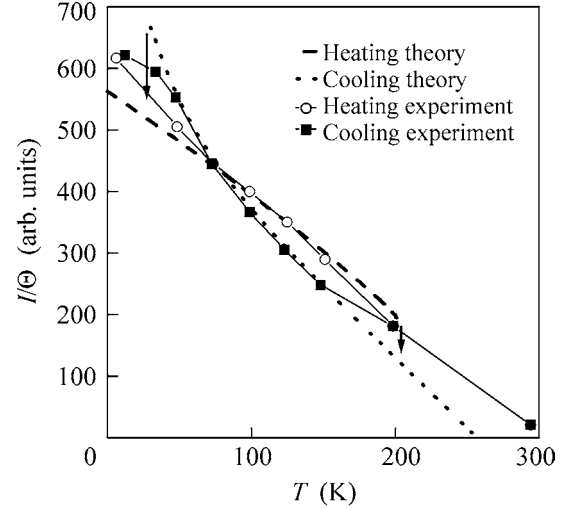


Fig. 2. Hysteric behavior of the reduced integrated intensity of Raman scattering for a line at frequency 50 cm^{-1} in a single crystal of $\text{Ba}_{0.67}\text{K}_{0.33}\text{BiO}_3$; $B = 4.6 \text{ eV \AA}^{-4}$, $v = 3.11 \text{ eV \AA}^{-2}$, $\lambda_k^{(3)} = 1.65 \text{ eV \AA}^{-3}$, $\lambda_{kk}^{(4)} = 1.24 \text{ eV \AA}^{-4}$, $\alpha = 3.69 \times 10^1 \text{ eV \AA}^{-2}$, $\beta = 7.5 \times 10^2 \text{ eV \AA}^{-3}$, $\gamma = 3.3 \times 10^3 \text{ eV \AA}^{-4}$, and $M_{\text{eff}} = 800m$, where m is the mass of an oxygen atom.

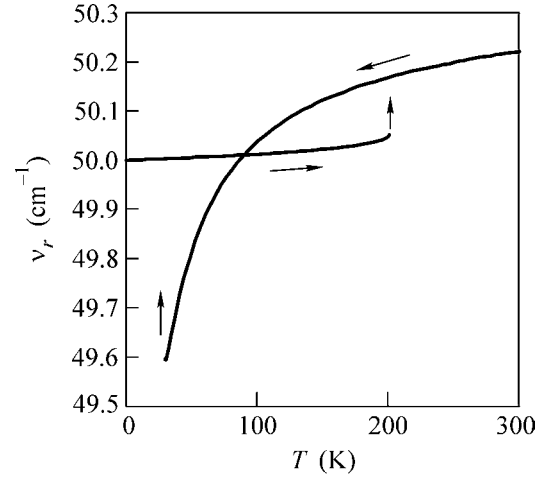


Fig. 3. Temperature dependence of renormalized frequency ν_r plotted in accordance with formula (4).

quency v_o because of interactions $H_{\text{int}}^{(3)}$ and $H_{\text{int}}^{(4)}$ (see Fig. 3). It should be recalled that these interactions represent the nonlinear relations between rotational vibrations of octahedra with the breather-type vibrations of oxygen ions in a two-well potential in the [100] direction. The inclusion of the contribution from $H_{\text{int}}^{(3)}$ or from $H_{\text{int}}^{(4)}$ alone leads to a simple (one-loop) hysteresis: the intensity of scattered light in the bistability region is lower for sample cooling and higher for sample heating

if $H_{\text{int}}^{(3)}$ is taken into account. If only $H_{\text{int}}^{(4)}$ is taken into consideration, the circumvention of the hysteresis curve is inverted (i.e., the cooling curve lies above the heating curve). The competition of the contributions from $H_{\text{int}}^{(3)}$ (with a minus sign, since this contribution differs from zero in the second order of perturbation theory) and from $H_{\text{int}}^{(4)}$ (with the plus sign if $\lambda_{kk}^{(4)} > 0$) forms the hysteresis curve of the two-loop type.

Thus, the presence of a phonon line of frequency 50 cm^{-1} in the Raman spectrum of a single crystal of superconducting oxide $\text{Ba}_{1-x}\text{K}_x\text{BiO}_3$ and the bistable temperature dependence of its integrated intensity reflect a number of features of the local lattice and electronic structures of this compound. First, this line emerges due to rotation of soft and hard BiO_6 octahedra. Rotational distortions are realized in the form of a local phase transition of the displacement type in the cooperated complex of hard octahedra, which may exchange their roles with soft octahedra owing to breather-type vibrations of oxygen ions in a two-well potential. Second, the integrated intensity of Raman scattering for this line decreases upon sample heating and vanishes at the critical temperature T_o of a local phase transition of the displacement type (i.e., in the case when cooperated coherent vibrations of the complex of octahedra are disrupted and local distortions in the cubic perovskite structure disappear). Third, the temperature hysteresis of the integrated intensity is due to the asymmetric nature of the dependence of rotational vibrations of octahedra with renormalized frequency ν_r on two nonequivalent positions of the oxygen ion transferring an electron pair from a soft to a hard

octahedron. The bistable behavior of this ion in the two-well potential is ensured by the cooperative behavior of the complex of octahedra; in addition, the competition of the contributions from interactions $H_{\text{int}}^{(3)}$ and $H_{\text{int}}^{(4)}$ to ν_r forms a hysteretic curve of the two-loop type for the temperature dependence of the intensity.

REFERENCES

1. A. P. Menushenkov, K. V. Klementev, A. V. Kuznetsov, and M. Yu. Kagan, Zh. Éksp. Teor. Fiz. **120**, 700 (2001) [JETP **93**, 615 (2001)].
2. Yu. G. Pashkevich, V. P. Gnezdilov, A. V. Eremenko, *et al.*, Int. J. Mod. Phys. **14**, 3637 (2000).
3. S. Zherlitsyn, B. Lüthi, V. Guzakov, *et al.*, Eur. Phys. J. **16**, 59 (2000).
4. D. E. Cox and A. W. Sleight, Acta Crystallogr. **35**, 1 (1989).
5. Shiyu Pei, J. D. Jorgensen, B. Dabrowski, *et al.*, Phys. Rev. B **41**, 4126 (1990).
6. Y. Yacoby, S. M. Heald, and E. A. Stern, Solid State Commun. **101**, 801 (1997).
7. M. Braden, W. Reichardt, W. Schmidbauer, *et al.*, J. Supercond. **8**, 595 (1995).
8. A. P. Menushenkov, K. V. Klement'ev, P. V. Konarev, and A. A. Meshkov, Pis'ma Zh. Éksp. Teor. Fiz. **67**, 977 (1998) [JETP Lett. **67**, 1034 (1998)].
9. A. P. Saiko and V. E. Gusakov, Zh. Éksp. Teor. Fiz. **116**, 168 (1999) [JETP **89**, 92 (1999)]; Zh. Éksp. Teor. Fiz. **108**, 757 (1995) [JETP **81**, 413 (1995)].
10. A. P. Saiko and S. A. Markevich, Pis'ma Zh. Eksp. Teor. Fiz. **78**, 782 (2003) [JETP Lett. **78**, 332 (2003)]; cond-mat/0309649.